Journal of Materials Chemistry B

Accepted Manuscript

ROYAL SOCIETY OF CHEMISTRY

www.rsc.org/materialsB

A highly bioactive and biodegradable poly(glycerol sebacate)-silica glass hybrid elastomer with tailored mechanical properties for bone tissue regeneration

Xin Zhao[a], Yaobin Wu[a], Yuzhang Du[a], Xiaofeng Chen [c], Bo Lei [a, c*], Yumeng Xue [a], Peter X Ma [a, b, d, e, f*],

[a] *Frontier Institute of Science and Technology, Xi'an Jiaotong University, Xi'an, China*

[b] *Department of Biologic and Materials Sciences, University of Michigan, Ann Arbor, USA*

[c] *National Engineering Research Center for Tissue Restoration and Reconstruction, Guangzhou, China*

[d] *Department of Biomedical Engineering, University of Michigan, Ann Arbor, USA*

[e] *Macromolecular Science and Engineering Center, University of Michigan, Ann Arbor, USA*

[f] *Department of Materials Science and Engineering, University of Michigan, Ann Arbor, USA*

*Corresponding author:

B Lei, rayboo@xjtu.edu.cn or leiboaray@gmail.com, Tel. +86-29-83395361

Abstracts

Biodegradable poly (glycerol sebacate) (PGS) elastomers have achieved much attention as promising materials for potential applications in soft tissue repair and regeneration, due to their biomimetic viscoelastic properties. However, the low strength and absence of bioactivity limited their potential applications in hard (bone, tooth, tendon and ligament) tissue regeneration. Here, we introduced the molecular-level silica bioactive glass into matrix of polymer elastomers to prepare bioactive hybrid elastomers (PGSSC) for bone tissue regeneration applications. We have shown here that our PGSSC provide some advantages over conventional bioactive materials and elastomers due to their controlled biomineralization (apatite-forming bioactivity), tunable elastic properties and biodegradation, enhanced osteoblasts proliferation. The tensile strength and initial modulus of PGSSC hybrid elastomers ranged from 1-5 MPa, 2-32 MPa respectively by controlling silica phase contents, which are several times higher than pure PGS elastomers. PGSSC elastomers also showed enhanced hydrophilicity with contact angle

range from 75 to 25 degree. The biological apatite was formed on surfaces of PGSSC when soaking in simulated body fluid (SBF) for 1 day. The osteoblast (MC3T3) demonstrated significantly enhanced proliferation on PGSSC compared with PGS. The development of bioactive PGSSC hybrid elastomers may offer a new choice for bone tissue repair and regeneration.

Keywords: Biomaterials; Silica bioactive glass; Elastomer; Hybrids; Bioactivity; Biocompatibility

1. Introduction

Most of human native tissues such as muscle, tendon, ligament and skin possess highly elastic properties (resilience and stretchability). Due to the biomimetic viscoelastic properties, biodegradable polymer elastomers have attracted much attention in tissue repair and regeneration[1-4]. Poly (glycerol sebacate) (PGS) elastomer, as a soft and elastic polyester, has been developed in recent years for soft tissue regeneration applications such as nerve guides and small diameter blood vessels[5-8]. This polymer shows a chemically cross-linked structure which could provide elastic recovery after loads. However, the mechanical properties of reported PGS elastomer usually range from 0.25 to 1.45 MPa (elastic modulus) and 0.3-1.5 MPa (tensile strength)[8, 9], which limited their potential applications in hard tissue regeneration such as bone, cartilage, tendon and ligand. The PGS elastomers also have other shortcomings in bone tissue regeneration applications, including poor hydrophilicity and low bioactivity (apatite-forming ability and cellular biocompatibility) [10].

To improve the applied range of PGS elastomers, several strategies have been previously reported to enhance their mechanical strength, hydrophilicity and biocompatibility. For example, various ceramic fillers, such as nano-fumed silica (with diameters around 25–35 nm), bioglass and halloysite, have been added into PGS elastomers to enhance their structure and properties[6, 11]. The incorporation of bioglass and halloysite could increase the mechanical properties and decrease the acidic products of PGS degradation, but the tensile strength and modulus of PGS-ceramic composite elastomers were still in a limited value below 1.6MPa. Wu [12] et. al. prepared a

silica nanoparticles filled poly(glycerol-sebacate-citrate) elastomers with the highest tensile strength of 5.3 MPa and improved cell biocompatibility. However, the addition of ceramic particles beyond size of several hundred nanometers may decrease the structure uniformity and result in unstable mechanical properties after transplantation *in vivo*. Therefore, development of molecular-level based ceramic-added PGS hybrid elastomers may be an important strategy for improving PGS mechanical strength and structure uniformity[13]. On the other hand, for successful bone tissue regeneration application, high biomineralization ability (apatite-forming bioactivity) is very necessary, which not only improves bone integration but also bone regeneration ability[14-16]. However, few studies reported the fabrication and apatite-forming bioactivity of molecular-based inorganic filler-PGS hybrid elastomers.

Silica-based bioactive glasses (SBG) have achieved successful applications in bone tissue repair and regeneration, due to their high osteoconductivity, osteoproductivity and gene-active properties[17-21]. Compared to conventional melting method, sol-gel derived SBG presented uniform chemical structure and high bioactivity *in vitro* and *in vivo*[22-26]. To optimize the properties for bone regeneration, as bioactive agents, sol-gel derived SBG microscale and nanoscale particles have been utilized to prepare polymer composites[27-29]. To further improve the chemical structure and tailor properties of composites, softened bioactive glass sol, possessing a molecular-level composition, has been previously reported to fabricate bioactive inorganic-polymer hybrid biomaterials[21, 30, 31]. For instances, gelatin, chitosan and collagen-silica-based hybrid materials have been fabricated successfully. The addition of silica phase significantly enhanced the mechanical properties, biomineralization and osteoblasts biocompatibility of polymer matrix [32-36].

Given the special advantages of silica-based bioactive glass and PGS elastomer, here we develop a PGS-Silica bioactive glass hybrid elastomers (PGSSC) by a direct hybridization method (organic and inorganic phase). It is hypothesized that silica-based glass phase can be dispersed in PGS matrix at a molecular level and its addition can significantly improve mechanical properties, hydrophilicity, biomineralization bioactivity, osteoblast

biocompatibility. It is anticipated that our PGSSC hybrid elastomers could find valuable applications in bone tissue regeneration.

2. Materials and methods

2.1 Synthesis of poly (glycerol sebacate) (PGS) pre-polymer

The PGS pre-polymer was synthesized by polycondensation of equimolar glycerol (Sigma-Aldrich) and sebacic acid (J&K) according to a previously published method with a slight modification[9]. Briefly, equimolar glycerol and sebacic acid were melted and stirred at 120°C under nitrogen for 24h and continued for another 36 h under vacuum. The pre-polymers were collected and used without any further purification.

2.2 Preparation of PGS and PGS/silica bioactive glass (PGSSC) hybrid elastomers

The PGS and PGSSC (C represents as Ca) hybrid elastomers films were fabricated based on the precursor solution hybridization, solvent evaporation and thermal curing process under vacuum. Silica-based bioactive glass sol was prepared according to our previously reported method [26]. Briefly, bioactive silica-based sol was formed by mixing 4 ml tetraethoxysilane (TEOS, J&K), 2.8 ml ethanol and 1.4 ml 0.1 M HCl with constant stirring for 3 hours at room temperature. PGS pre-polymer was dissolved in ethanol to form a 15 wt% solution. Bioactive glass sol was formed by adding calcium chloride into silica sol. The final solution possessed a Si/Ca mol ratio of 3:2. The PGSSC hybrid solution was fabricated by adding different amount of inorganic sol into pre-polymer solution. Typically, to prepare PGS15Si10Ca, 5.3 ml 15wt% pre-polymer solution, 0.9 ml silica sol and 47.5 mg calcium chloride were mixed and stirred at 60℃ for 1.5 h. 15Si means the volume percent of TEOS in total pre-polymer solution. Then, the mixture was cast into the Teflon dish and dried in an oven at 60℃ for 24 h to slowly evaporate the solvents. To obtain PGS and PGSSC hybrid elastomers, the Teflon dish was transferred to the vacuum oven and thermally cured at 140℃ for 36 h. The PGSSC hybrid elastomers with other compositions were prepared by the same method. The samples codes and composition were shown in Table 1.

2.3 Physicochemical structure characterizations of pre-polymer and elastomers

The average molecular weight of PGS pre-polymer was determined using gel permeation chromatography (GPC,Waters-2414,Waters).The chemical structures of PGS pre-polymer (mushy form), PGS and PGSSC hybrid elastomers (films) were recorded using Fourier Transform Infrared spectra (FTIR, NICOLET 6700, Thermo). The spectra were collected at 4 cm resolutions with average value of 32 scans. The molecular structure of PGS pre-polymer was also analyzed using Nuclear Magnetic Resonance (^{1}H NMR) spectroscopy (^{1}H NMR, AVANCE IIIHD400, Bruker). Briefly, the pre-polymer sample was dissolved in $CDCl_3$ and the spectrum was recorded at 400 MHz. The resulting datum was processed and analyzed using Topspin software. The peak assignments in the NMR spectrum for PGS pre-polymer are listed below. ^{1}H NMR (PGS) (400 MHz, CDCl3) d/ppm: 1.30 (37H, m, -C$\underline{H}_2$-), 1.62 (18H, d, -C$\underline{H}_2$CH$_2$O(CO)-), 2.35(18H, m, -C$\underline{H}_2$O(CO)-), 3.50-3.85 (6H, m, OHC$\underline{H}_2$CHO-), 3.94 (1H, m, -OCH$_2$C$\underline{H}$OH), 4.05-4.35 (15H, m, -OC$\underline{H}_2$CHO-), 5.09 (1H, s, OHCH$_2$C$\underline{H}$O-), 5.26 (1H, s, -OCH$_2$C$\underline{H}$O-). The crystalline phase structure was determined by X-ray diffraction spectroscopy (XRD, SMART APEX-2 CCD, BRUKE) measurements.

2.4 Mechanical behavior of PGS and PGSSC hybrid elastomers

Uniaxial tensile mechanical properties of PGS and PGSSC hybrid elastomers were performed on an instron Materials Test system (MTS Criterion 43, MTS Criterion) equipped with a 50 N load cell. Before tensile test, thermally crosslinked samples were cut into a rectangular shape with 8 mm in length and 3 mm in width. The uniaxial tensile testing was performed at a jog rate of 20 mm/min until sample failure at 25 ^{o}C with a relative humidity of 20 %. The tensile stress-strain curves were obtained from force-displacement curves recorded by system software. The tensile strength (MPa) were obtained by dividing the applied force (N) with cross section area (mm^2). Young's modulus (MPa) of samples were obtained by calculating the slope of stress-strain curves between 5% - 15% strain. To obtain mean value and standard deviation, at least three species for each sample were tested.

2.5 Hydrophility and hydration ability evaluation of PGS and PGSSC elastomers

The hydrophility of samples was evaluated by dynamic water contact angle measurement (SL200KB, Kono). Before test, the elastomer films were cut into a size of 10 mm×40 mm. To test the water contact angle, a droplet of deionized water was deposited on the surfaces of samples using 21-gauge needle. After 2 min, the water contact angles were calculated and high-resolution image was captured. At least five positions for each sample were measured. For hydration kinetic studies, samples with a size of 4 mm diameter and initial weight of W_0 were soaked in phosphate buffer saline (PBS) at physiological conditions (37℃). At regular time intervals, the swollen samples were taken out, blotted with a filter paper to remove excess surface water, and their swollen weights (Ws) were recorded. The water uptake by the polymeric network was determined by Eq. (1) as follow.

$$\text{Water uptake}\ (\%) = \frac{Ws - Wo}{Wo} \times 100 \quad (1)$$

2.6 In vitro degradation studies of PGS and PGSSC hybrid elastomers

Degradation studies of PGS and PGSSC hybrid elastomers were evaluated by alkaline degradation (0.08M NaOH solution) at 37℃. The alkaline solution was used to evaluate the polymer degradation ability in a relatively short period of time. Before test, the elastomer films were cut into discs with a 4 mm diameter using a cork borer. Briefly, the samples were placed in test tubes containing 10 ml of 0.08 M NaOH solution, incubated at 37℃for different period of times (4 days for NaOH solution). At least 3 species for each sample were tested. The initial weights of the samples were noted as W_0. At pre-set time points, samples were removed and washed thoroughly with deionized water (3 times) and dried at 60ºC until constant weight. The final dry weight was denoted as W_t. Degradation was measured by determining the mass loss of the samples over the period of the study, as shown in Eq. (2).

$$\text{Mass loss}(\%) = \frac{Wo - Wt}{Wo} \times 100 \quad (2)$$

2.7 Thermal properties of PGS and PGSSC hybrid elastomers

Thermal degradation and stability measurements of elastomers were performed with a Thermogravimetric Analysis instruments (TGA, TGA-2950, TA) in a nitrogen atmosphere at a heating rate of 10℃/min from 30 ℃ to 700℃. Data were reported and analyzed by Universal Thermal Software. The thermal physical properties were determined by a Differential Scanning Calorimetry (DSC, DSC-2920, TA). At a nitrogen flow rate of 30 mL/min, samples were first heated to 250 ℃and cooled to -60℃ at the rate of 10℃/min to get homogeneous thermal history, and then heated to 250℃ at the rate of 10℃/min. Data reported herein on the thermal transitions were obtained from the second heating scans and analyzed/calculated by Universal Thermal Software.

2.8 Biomineralization bioactivity in vitro of PGS and PGSSC hybrid elastomers

The *in vitro* biomineralization bioactivity of hybrid elastomers was determined by evaluating the apatite-forming ability on their surfaces after soaking in simulated body fluid solution (SBF). The SBF solution has a similar chemical composition with blood plasma and was prepared according to our previous report [18]. The elastomer films were immersed in SBF solution with a concentration of 1.5 mg/ml, located in a shaking air bath at 37 ^{o}C for 1 day and 7 days. The SBF solution was refreshed every other day. After soaking, samples were removed from the SBF solution, gently washed with distilled water, and then dried at room temperature. The apatite-forming ability on materials surfaces was evaluated as changes of surface morphology, surface composition and crystalline structure before and after soaking in SBF. These changes were monitored by field emission scanning electron microscopy (FE-SEM, JSM6701F, JEOL) with energy dispersed spectroscopy (EDS) capability, X-ray diffraction spectroscopy (XRD, SMART APEX-2 CCD, BRUKE) and FTIR spectra (FTIR, NICOLET 6700, Thermo) measurements. Prior to the SEM observations, samples were coated with a thin layer of Au using a sputter coater at a pressure of 32 mTorr for 150 s.

2.9 Cellular biocompatibility in vitro of PGS and PGSSC hybrid elastomers

The cell biocompatibility of elastomers was studied using osteoblast cell line (MC3T3-E1) as a model. Cell

proliferation was carried out by a commercial AlamarBlue™ assay kit (Life Technologies). Before cell culture, elastomers films were coated on coverslips with 14 mm diameter. Prior to cell culture, samples were sterilized with 75% ethanol for 2 h and ultraviolet (UV) irradiation for 30 min. The materials were placed in 24-well culture plate and cells were seeded on surfaces of samples with a cell density of 4000 cells/ well. Cell was incubated at 37 ^{o}C in a humidified atmosphere with 5% CO_2. After culture for 1 and 3 days, 100 μL of AlamarBlue™ indicator was added to each well and incubated for 4 h. Then, 100 μL of the medium in each well was added into a 96-well black plate (Costar). Fluorescence intensity was recorded by a microplate reader (SpectraMax i3, Molecular Devices) according to the instruction book. At least 4 species for each sample were tested. Cell proliferation was quantified by the percentage reduction of AlamarBlue™. For observing the cells adhesion and morphologies, live/dead viability kit (Molecular Probes) assay was employed. Also the cells adhered onto the films surfaces were observed using inverted phase contrast microscope (CH20, Olympus). At the pre-determined time, samples with cells were washed by PBS and stained using a live/dead viability kit according to the instruction. The fluorescent morphologies of cells were observed under an inverted fluorescence microscope (IX53, Olympus).

2.10 Statistics

Experimental data were presented as mean±standard deviation (SD). Statistical differences between experimental groups were analyzed using T-Test analysis. Statistical significance was represented as *$p<0.05$ and **$p<0.01$.

3. Results and discussion

3.1 Fabrication of poly (glycerol sebacate)-silica bioactive glass (PGSSC) hybrid elastomers

Silica-based bioactive glass (SBG) nanoparticles and molecular-level sol have been previously reported to prepare bioactive polymer hybrid biomaterials for bone tissue repair and regeneration. The addition of silica phase could efficiently improve the mechanical properties and biominerialization activity of biomedical polymer. Here,

we incorporated silica-based bioactive sol into poly (glycerol sebacate) (PGS) elastomers by direct hybridization method, as shown in Fig.1. PGS elastomers were synthesized by conventional thermal polymerization technology based on the reaction between glycerol and sebacate acid (Fig.1A). SBG sol was prepared by acid-catalyzed sol-gel reaction of tetraethyl orthosilicate and calcium precursors. Due to similar solubility in ethanol-water system, SBG sol could be hybridized with PGS pre-polymer solution at a molecular-level (Figs.1B-C). In this hybridization process, silica micelles were dispersed in PGS chain, and the hydrogen bond interaction between Si-OH and –OH of PGS polymer chain may happen. This hybridized structure was kept and formed to be PGS-silica bioactive glass (PGSSC) hybrid elastomers after thermal curing. The fabrication process of hybrid elastomers included hybrid solution sol-gel reaction, solvents evaporation and thermal curing under vacuum. The final PGSSC hybrid elastomers still showed transparent feature (Fig.1D), indicating their molecular-level distribution in PGS matrix.

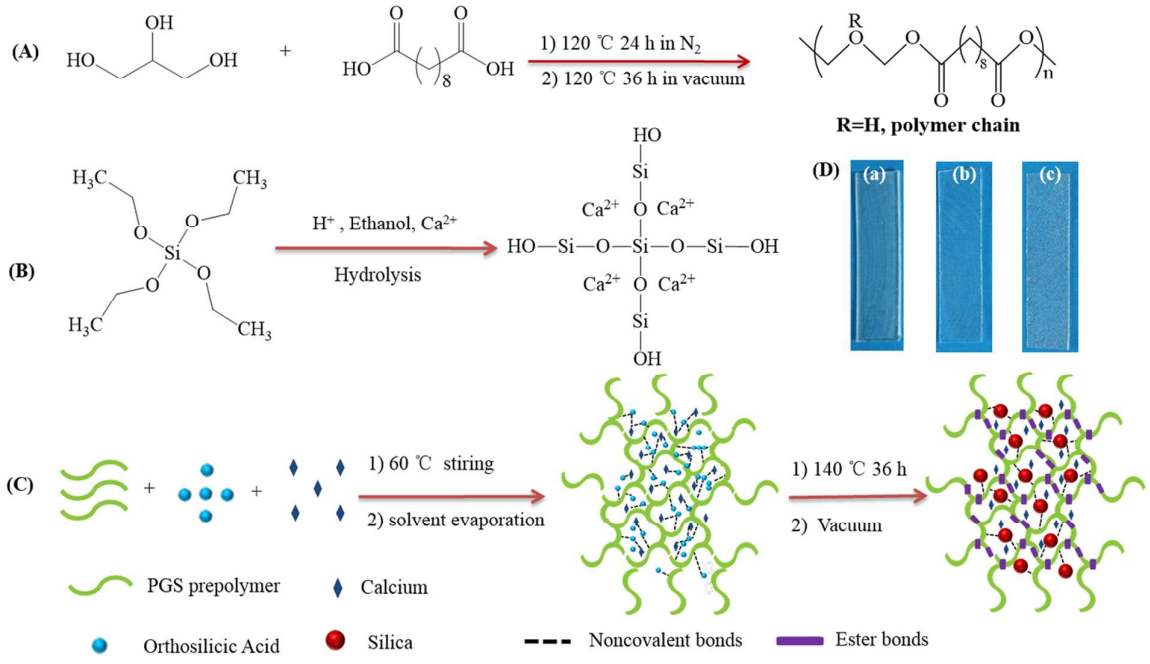

Figure 1. Scheme illustration for preparing PGSSC hybrid elastomers. (A) synthesis of PGS pre-polymer; (B) formation of silica-based bioactive glass sols; (C) fabrication of PGSSC hybrid elastomers; (D) optical images of PGS and PGSSC hybrid elastomers (a: PGS; b: PGS15Si; c: PGS20Ca).

3.2 Physicochemical structure of PGS and PGSSC hybrid elastomers

The molecular structure of PGS pre-polymer was determined by H^1NMR spectroscopy, as shown in Fig. 2A. In the H^1NMR of PGS pre-polymer, the peaks identified at 1.30, 1.62 and 2.35 ppm were assigned to methylene peaks related to sebacic acid, whereas peaks related to glycerol were identified between 4.05-4.35 ppm and 5.05-5.30 ppm. This result was consistent with previous report [37]. The gel permeation chromatography (GPC) indicated that synthesized pre-polymer presented an average molecular weight (Mw) of 33707 g/mol with a polydispersity index (PDI) of 1.65. Furthermore, the chemical structure of PGS pre-polymer was further investigated by FTIR, as shown in Fig.2B. A strong peak around 1735 cm^{-1} corresponding to the ester group related to backbone of PGS was observed. These results indicated that the PGS pre-polymer was synthesized successfully by the thermal polymerization method.

The FTIR spectra of PGS and PGSSC hybrid elastomers after thermal curing are shown in Figs.2B-C. The absorption peaks at 1000-1100 cm^{-1} can be attributed to the asymmetric stretching vibration of Si-O-Si groups, which provided evidence of a successful condensation reaction between Si-OH groups under high temperature [38, 39]. This result also indicated the formation of silica-based glass network after thermal cross-linking. In addition, the absorbance peak of Si-O-Si became larger with an increase of silica content from 5 to 15 wt% (PGS5Si, PGS10Si, PGS15Si, PGS15Si10Ca, PGS15Si20Ca). No significant difference for FTIR spectra was observed when calcium was incorporated in PGS-Si elastomers. Wide-angle X-rays was used to investigate the effect of silica phase incorporation on crystal structure of PGS elastomer (Fig.2D). PGS elastomer showed a broad and weak peak at 22° and 45° suggesting its representative amorphous structure. Actually PGS-based elastomers have been widely accepted as amorphous structures although several broad peaks usually presented in their XRD spectra [40, 41]. The incorporation of silica and calcium phase did not produce significant effect on the crystalline phase structure of PGS (Fig.2D). Our results were also consistent with previous reports about PGS elastomers [40, 41].

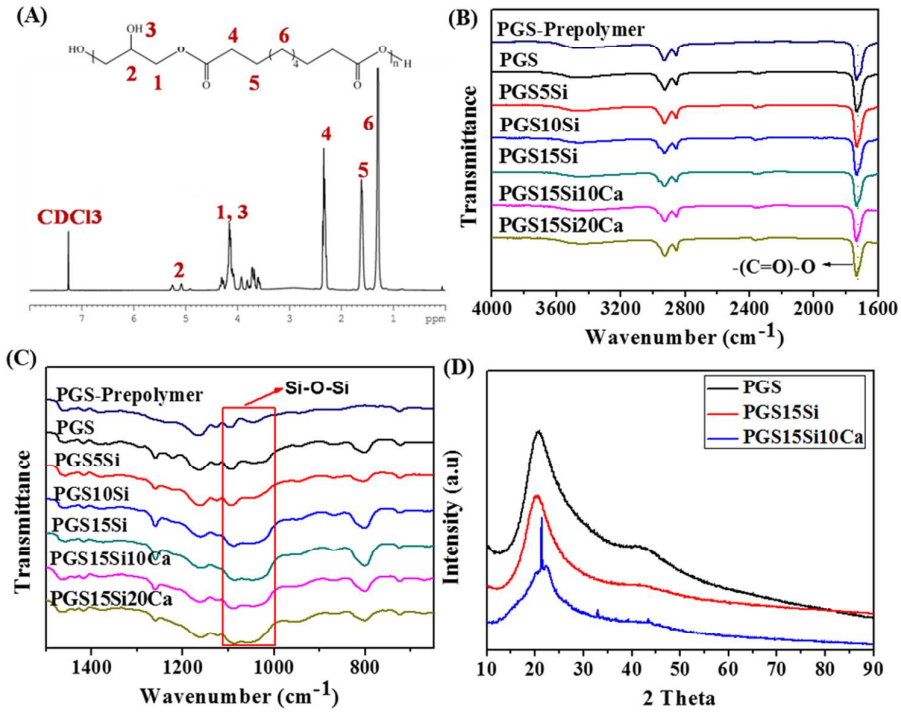

Figure 2. Chemical and crystal structure of PGSSC hybrid elastomers. (A) H^1 NMR spectrum of synthesized PGS pre-polymer showing the typical molecular structure of PGS; (B, C) FTIR spectra of PGS pre-polymer and PGSSC hybrid elastomers after thermal curing, indicating the formation of polyester structure and silica network; (D) XRD analysis of PGS and PGSSC hybrid elastomers, demonstrating their poor-crystal or amorphous structure.

Figure 3 shows the surface morphology and composition of the PGS and PGSSC hybrid elastomers, respectively. Pure PGS elastomer showed a relatively smooth surface with a corrugated morphology (Fig.3A). This corrugated microstructure may be due to the electron beam irradiation under high magnifications. As the addition of silica phase, there was no significant change about the surface of elastomer compared with PGS elastomer (Fig.3B). When calcium was introduced into PGS-Silica matrix, the significantly high roughness was observed (Fig.3C). The enhanced surface roughness can be assigned to the phase separation of inorganic phase in PGS polymer matrix and this phase separation might be due to the poor interaction between Ca and polymer chain under treatment of high temperature. The presence of the silica phase and calcium phase in the hybrid elastomers were confirmed by EDS

analyses, as shown in Fig.3. As compared to PGS elastomer, the PGS15Si hybrid film showed strong peak corresponding to Si element, and the PGS15Si10Ca hybrid film exhibited the characteristic peaks related to Si and Ca elements.

These results including H^1NMR, FTIR, SEM, EDS, XRD suggest that homogeneously hybridized PGSSC elastomers could be fabricated successfully by the solvent evaporation method combined with the silica-based sol–gel process.

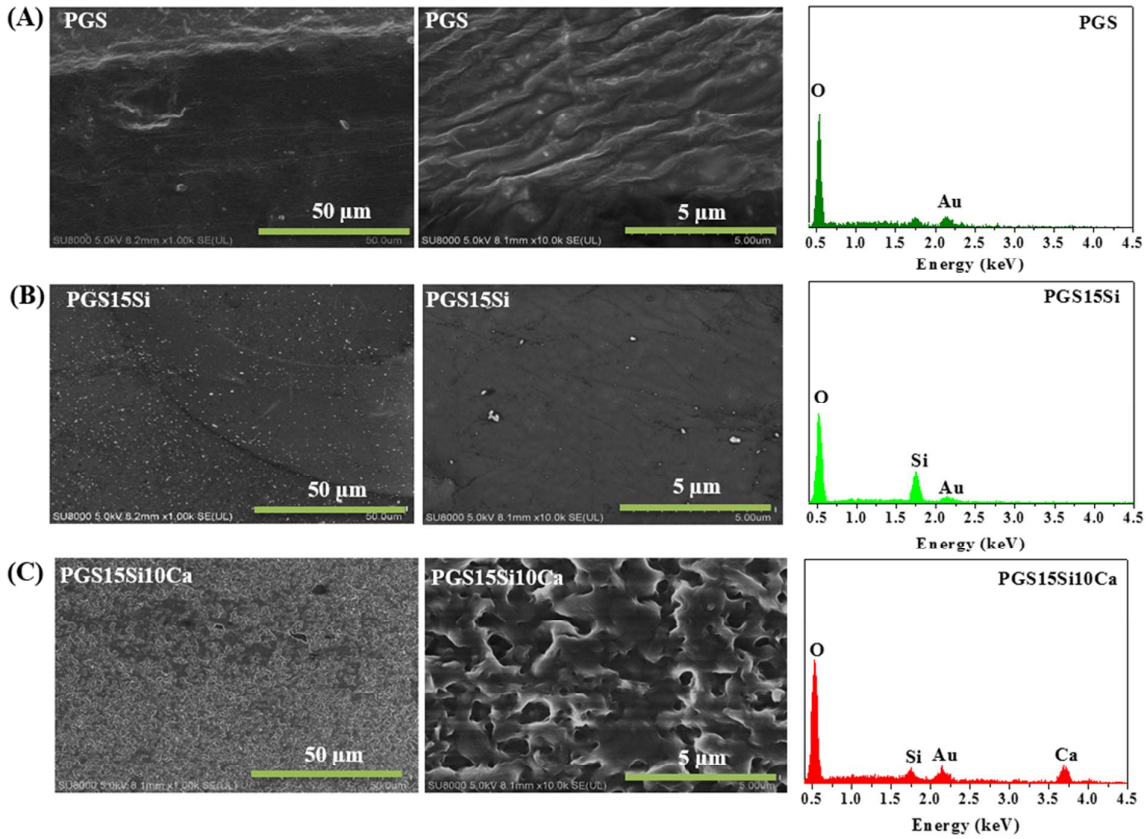

Figure 3. Surface morphology and composition of PGSSC hybrid elastomers. (A-C) SEM images and EDS analysis of PGS (A), PGS15Si (B), PGS15Si10Ca (C).

3.3 Thermal properties of PGS and PGSSC hybrid elastomers

The effect of silica phase incorporation on thermal stability of elastomers is shown in Fig.4. Fig.4A and Fig.4B present the differential scanning calorimetry (DSC) and thermo-gravimetric analysis (TG) results of PGS and

PGSSC hybrid elastomers, respectively. The DSC analysis could efficiently determine the exothermic-endothermic changes and phase transformation of elastomer materials[42]. It was shown that all elastomers exhibited endothermic peaks and glass transformation temperature (T_g). As shown in Fig.4A, PGS, PGS15Si and PGS15Si10Ca elastomers showed a T_g of -20.0, -24.8 and -25.01°C, respectively. The addition of silica phase decreased the T_g of PGS elastomers, which can be attributed to the reason that silica phase incorporation may decrease the polymer chain interactions thus facilitate the free movement of chains. Furthermore, all elastomers showed the glass transformation temperature below 0°, indicating their rubbery states and amorphous structure at 37 °C [40, 41]. Those endothermic peaks presented between -10 and 10° should be attributed to the melting temperature of polymer, which was also consistent with previous report [8]**.** After the peaks, no any new endothermic and exothermic peaks were observed. However, the decreased DSC curves (endothermic direction) after endothermic peak may be ascribed to the slow decomposition which was also confirmed by TG curves (Fig.4B).

The thermal degradation behavior of PGS and PGSSC hybrid elastomers was also investigated by TG analysis, as shown in Fig.4B. The early mass loss occurred at about 291°C, 250°C, and 189°C respectively, which may be assigned to the loss of chemical combined water and decomposition of residual organic chemicals in elastomers. As the addition of silica and calcium phase, the decrease of weight loss temperature was probably due to the increased organic residues in inorganic sol and combined water (calcium chloride is easy to combine water) for PGS15Si and PGS15Si10Ca, respectively. The mass loss stage between 416°C and 700°C can be ascribed to degradation of polymer. The final residual weight percentages were 2.5, 13.9 and 19.5 wt% for the pure PGS, PGS15Si and PGS15Si10Ca elastomers, respectively. These results indicated that the actual weight contents of inorganic phase in elastomer were about 11.4% and 17% for PGS15Si and PGS15Si10Ca, respectively. The 2.5% residual for pure PGS might be attributed to carbon-related products formed at high temperature.

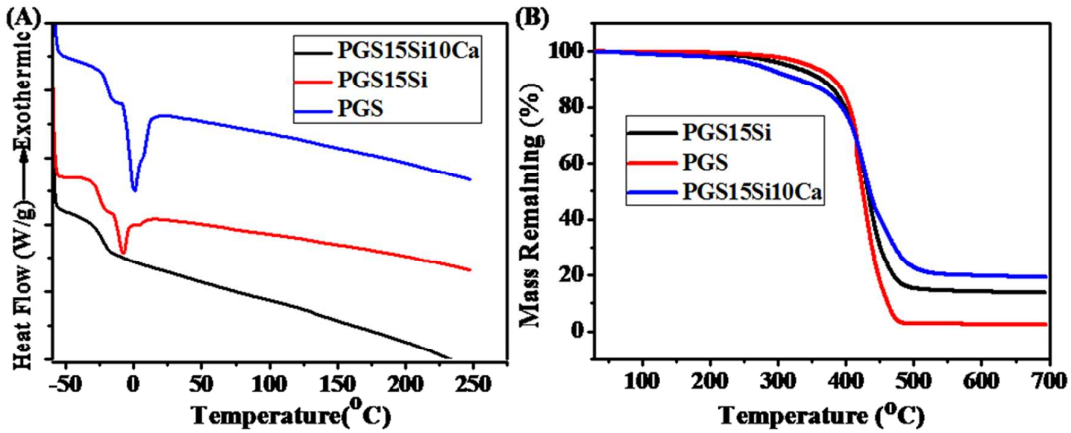

Figure 4. Thermal stability analysis of PGS and PGSSC hybrid elastomers. (A) DSC measurement showing the highly elastic feature at room temperature for all samples; (B) TG analysis indicating high thermal stability of hybrid elastomers above 400℃.

3.4 Mechanical behavior of PGS and PGSSC hybrid elastomers

It was well shown that addition of inorganic phase could affect mechanical behavior of polymer matrix[43]. Here we investigated the effect of silica and calcium phase incorporation on the tensile properties of PGS elastomers, as shown in Fig.5 and Table 1. The stress-strain curves of samples indicated that all synthesized elastomers showed the representative characteristic of elastomers (Fig.5). The tensile elastic behavior was enhanced with the addition of silica and calcium phase. As shown in Table 1, the ultimate tensile strength (UTS) and elastic modulus (EM) of samples were significantly increased as the improvement of silica and calcium contents. Compared to PGS elastomer, about 2 times (2.4 MPa) and 2.5 times (2.8MPa) improvement related to UTS was observed for PGS15Si and PGS15Si10Ca, respectively, although the fracture strain presented a decrease. Additionally, at least 10 times enhancement at EM (16 MPa and 20MPa) could be achieved for PGS15Si and PGS15Si10Ca, respectively. Our UTS and EM of hybrid elastomers was still higher than those of bioglass-PGS (1.5MP at UTS and 1.6 MPa at EM) and halloysite-PGS composites (1.6 and 1.5MPa)[11, 44]. The significant improvement of EM could be attributed to interaction mechanism between inorganic phase and polymer chain. In our study, silica phase could be dispersed

in PGS matrix at a molecular level. For PGS15Si, silica phase addition significantly increased the inorganic phase distributions in polymer matrix and thus improved the hybrid phase crosslinked density which increased the stiffness and modulus. For PGS15Si10Ca, in addition to the silica phase crosslinking effect, the ions bonds may be formed between Ca^{2+} and residual carboxyl groups from monomers of PGS, which further improved the crosslinked density of elastomers and thus enhanced the modulus.

The significant increase at modulus and decrease at strength was well known for most inorganic phase or particles reinforced materials systems [45]. In our study, silica-based sol possessed a molecular level distribution in PGS matrix, which can efficiently improve the ability resisting external force and then enhance the mechanical strength. It should be noted that the mechanical properties of elastomers may decrease under hydration condition. The previous studies have shown that mechanical strength of particles reinforced PGS elastomers had a decrease to some extent after hydration [44]. Our hybrid films were prepared by dispersing inorganic phase in polymer matrix at a molecular-level rather than a particle-level, which might lead to a strong interaction between organic and inorganic components. We speculate that the mechanical strength of our hybrid elastomers might decrease after hydration, but we believe that the hybrid films still have a higher mechanical strength than pure PGS film.

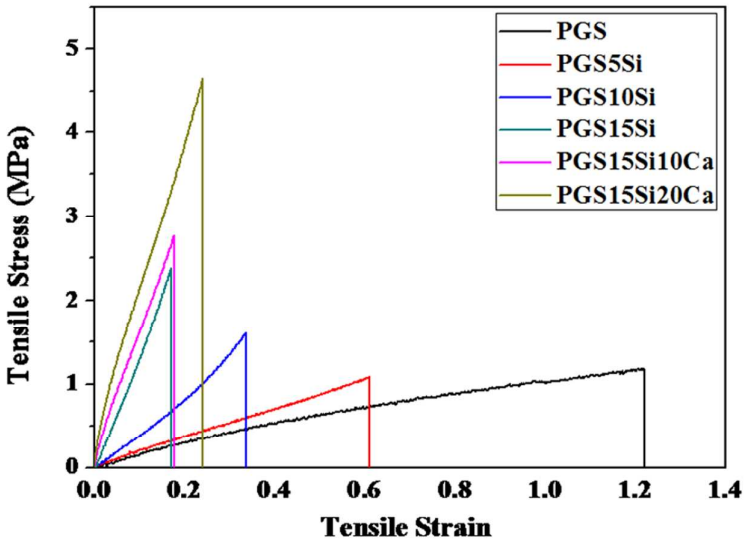

Figure 5. Representative tensile stress-strain behavior of PGS and PGSSC hybrid elastomers. All samples showed typical elastic mechanical behavior and tensile stress significantly increased as the incorporation of silica and calcium phase.

Table 1. Mechanical strength (tensile stress, fracture strain and elastic modulus) of PGS and PGSSC hybrid elastomers. ** $p<0.01$ means significant difference compared to PGS elastomers (n=4).

Samples	Ultimate Tensile Strength（MPa）	Fracture Strain（mm/mm）	Elastic Modulus (MPa)
PGS	1.13±0.10	1.05±0.15	1.75±0.15
PGS5Si	1.39±0.26	0.57±0.06	2.50±0.38 **
PGS10Si	1.65±0.17**	0.22±0.01	7.33±0.78**
PGS15Si	2.40±0.06**	0.14±0.01	16.75±0.21**
PGS15Si10Ca	2.79±0.10**	0.18±0.02	20.79±1.40**
PGS15Si20Ca	4.00±0.84**	0.21±0.03	34.52±4.73**

3.5 Hydration and biodegradation of PGS and PGSSC hybrid elastomers

It was well known that the hydrophilicity, hydration ability and degradation of biomaterials play an important role for their successful applications in biomedicine[46-48]. Here the hydration and degradation of PGS and PGSSC hybrid elastomers were investigated, as shown in Fig.6. Fig.6A shows the water contact angle result of samples.

Pure PGS elastomer presented a poor hydrophilicity with a water contact angle of 78°. Compared with PGS, silica phase incorporation, with a range of 5% to 15%, slightly enhanced the water contact angle, which was probably because there was no enough silica content in PGS matrix. However, once addition of calcium phase into PGS15Si, the water contact angle of the hybrid elastomers decreased significantly up to 37° and 28°. This result can be attributed to the high water absorption ability of calcium chloride.

The hydration properties of PGS, PGS15Si and PGS15Si10Ca elastomers were further evaluated by water uptake and equilibrium water content after soaking in PBS (Figs.6B-C). All samples reached a maximum water uptake after 7 hours soaking in PBS. Pure PGS elastomer only had a negligible water uptake within 7 hours, and the water uptake content significantly increased with addition of silica and calcium phase. PGS15Si and PGS15Si10Ca have an equilibrium water content of 16.9% and 28.0%, respectively. These results indicated that PGSSC hybrid elastomers possessed the high hydration ability for long term soaking. It also demonstrated that either silica or calcium phase addition can enhance the hydrophilicity of the PGS elastomers although initial water contact angle of PGS15Si was high. The degradability ability of PGS and PGSSC hybrid elastomers was investigated in 0.08 M sodium hydroxide solution, as shown in Fig.6D. The results indicated that PGSSC hybrid elastomers had a significantly high degradation rate in NaOH solution, as compared to PGS elastomers. After 50 hours soaking, beyond 90% of PGSSC hybrid elastomers had been degraded. The high degradation rate of silica and calcium-added samples should be attributed to their high hydration ability. Because high hydration ability would result in increased water uptake which can attack polymer chains and silica network, high weight loss was observed from PGSSC hybrid elastomers.

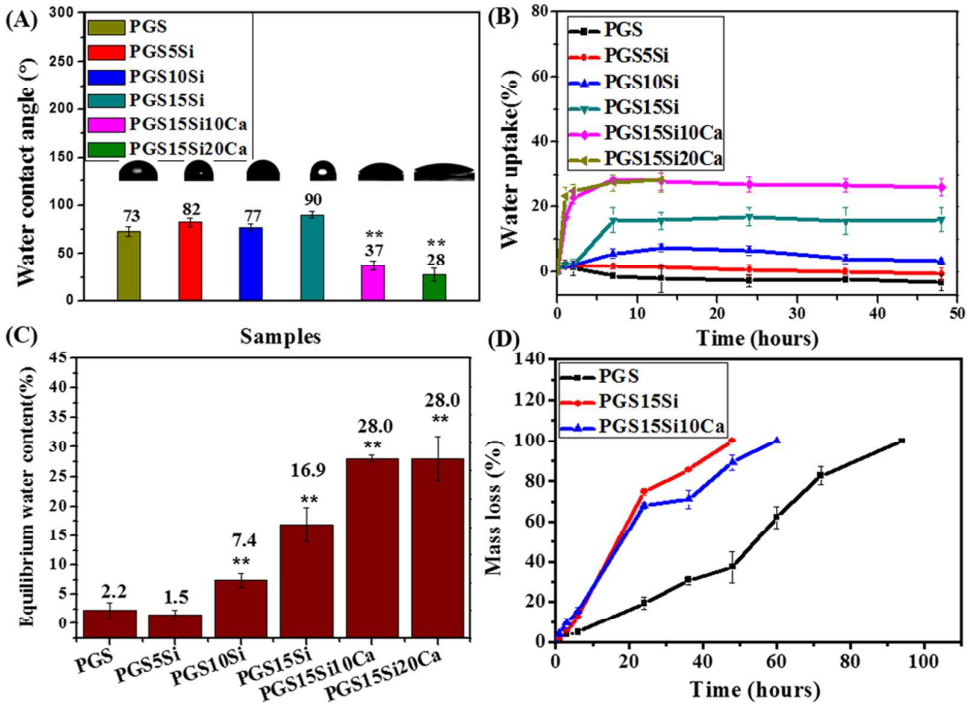

Figure 6. Hydrophilicity and degradation properties of PGS and PGSSC hybrid elastomers. (A) water contact angles test; (B) water uptake as soaking time in PBS; (C) equilibrium water content; (D) mass loss as soaking time in 0.08M NaOH. PGSSC hybrid elastomers showed significantly high hydration ability and degradation rate, as compared to PGS elastomer. ** $p<0.01$ means significant difference compared to PGS elastomers (n=4).

3.6 Biomineralization activity in vitro of PGS and PGSSC hybrid elastomers

In bone tissue repair and regeneration, enhanced osseointegration ability has a critical role on successful applications[49, 50]. Silica-based bioactive materials possess high biomineralization ability and biological apatite-forming activity which can significantly enhance bone-bonding or osseointegration ability[51]. Therefore, in this study, we investigated if silica/calcium phase hybridization could provide the biominerialization activity for PGS elastomers. Fig. 7 showed the surface morphology changes of PGS, PGS15Si and PGS15Si10Ca after immersing in SBF for 1 and 7 days. The surface of PGS elastomer did not have any change after 7 days soaking. However, compared to PGS, plate-shaped minerals with a thickness of 300-500 nm were observed on surface of PGS15Si and PGS15Si10Ca hybrid elastomers after 1 day soaking. After 7 days soaking, the deposition layer

increased and had covered the surfaces of materials.

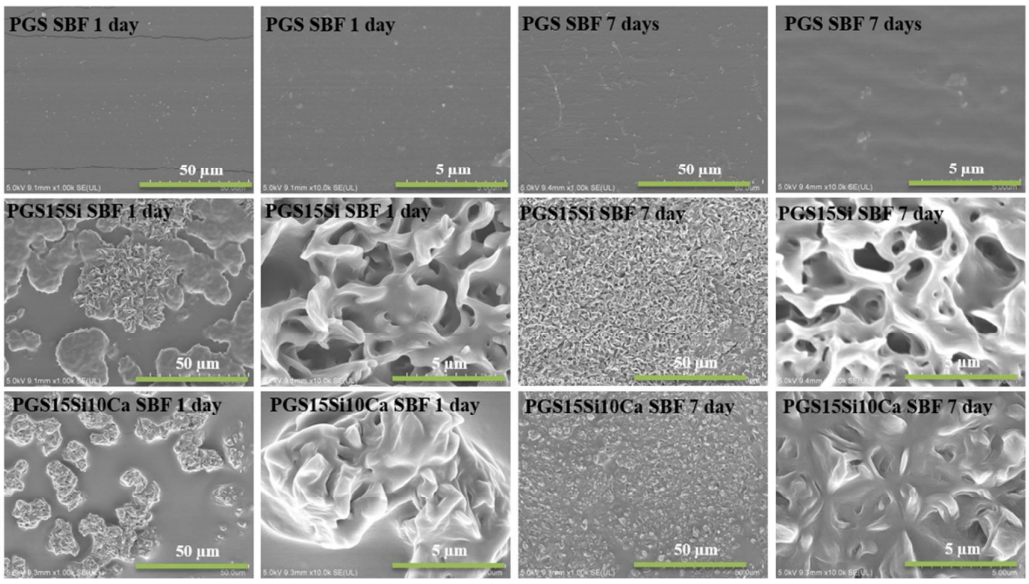

Figure 7. SEM images showing biomineralization activity of PGS and PGSSC hybrid elastomers. PGS, PGS15Si and PGS15Si10Ca hybrid elastomers were soaked in SBF for 1 and 7days. All PGSSC hybrid elastomers demonstrated high biomineralization ability after immersing in SBF as compared to PGS elastomers.

The EDS, XRD and FTIR were used to further determine the type of deposited minerals on surface of samples. As shown in Fig.8, after 7 day soaking, no any Ca and P peaks were observed from the EDS spectrum of pure PGS elastomer, suggesting no new formed minerals on their surfaces. However, the EDS spectra of PGS15Si and PGS15Si10Ca hybrid elastomers showed significant Ca and P peaks, indicating their Ca-P compositions of biominerals. Moreover, no any new peaks were observed from XRD spectra of PGS elastomers (Figure 9), while two new peaks at 32° and 46° were found from those of PGS15Si and PGS15Si10Ca hybrid elastomers. The new peaks identified at 32° and 46° were assigned to the 211 and 222 reflections of apatite (JCPDS 09-0432)[52, 53]. The characteristic peaks intensity for PGS15Si significantly increased as the extension of soaking time. The apatite peaks for PGS15Si10Ca seemed to be less distinct, indicating the formation of apatite with poor crystalline structure. This poor apatite crystalline phase was probably due to the high ions saturation resulted by quick calcium ion release in SBF solution. Due to the serious overlap of characteristic peaks between hybrid elastomers and

bio-mineralized apatite, the peaks intensity of HA in FTIR spectra at 562 cm^{-1} and 602 cm^{-1} was weak (Figure S1, supporting information). The results of SEM, EDS and XRD clearly showed that our hybrid elastomers could efficiently induce the formation of biological apatite compared PGS elastomers. The formation mechanism of apatite for our hybrid system could be attributed to the silicic acid layer formation of hybrids surface and Ca ion release from hybrid. The silicic acid layer could efficiently induce the deposition of Ca and PO_4^{3-} ions in SBF. In addition, Ca ion release from hybrid could also increase the supersaturation of medium towards apatite precipitation. This apatite formation mechanism was similar with class I and class II polymer-bioactive glass hybrids systems[26, 30, 32, 36].

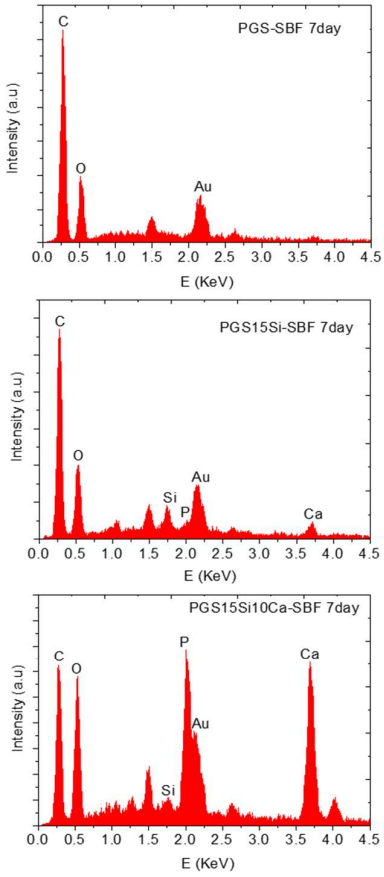

Figure 8. EDS analysis for biominerialized PGS and PGSSC hybrid elastomers. After soaking in SBF 7 days, PGSSC hybrid elastomers showed representative characteristic peaks of P and Ca attributed to the apatite as compared to PGS elastomers.

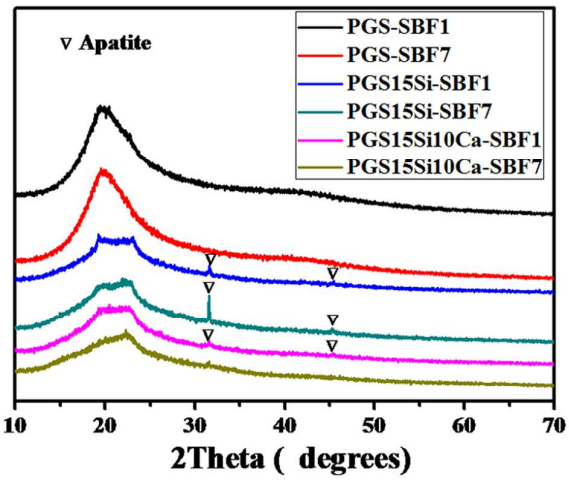

Figure 9. XRD patterns showing biomineralization activity of PGS and PGSSC hybrid elastomers. After soaking in SBF for 1 day and 7 days, PGSSC hybrid elastomers demonstrated representative characteristic peaks of apatite nanocrystals as compared to PGS elastomers.

3.7 Osteoblast biocompatibility in vitro of PGS and PGSSC hybrid elastomers

Based on the controlled mechanical properties and biomineralization activity, we also evaluated the effect of PGS and PGSSC hybrid elastomer on osteoblasts biocompatibility. Fig.10 exhibits the MC3T3 cell line proliferation on PGS and PGSSC hybrid elastomers after culture for 1 day and 3 days. Cells demonstrated the significant growth on all samples as the increase of culture periods. Significantly high cell metabolic activity on PGSSC (PGS5Si, PGS15Si) was observed at 1 day and 3 days, as compared to that on PGS. This result presented that PGSSC hybrid elastomers could significantly enhance osteoblast proliferation in comparison with PGS, indicating their high biocompatibility. In addition, as shown in Fig.11, the cell presented a normal spreading and morphology on the surfaces of hybrid elastomers after 3 day culture, suggesting good cell affinity of our materials. The osteogenic differentiation and bone tissue regeneration applications of PGSSC hybrid elastomers will be investigated in further studies.

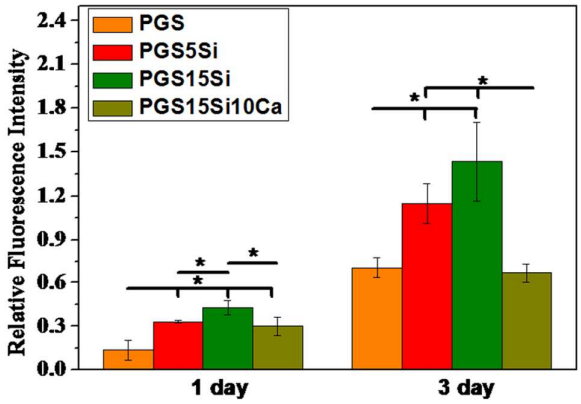

Figure 10. Cell proliferation of MC3T3 cells on PGS and PGSSC films with PGS served as the control group.

* $p<0.05$ means significant difference between the groups (n=4).

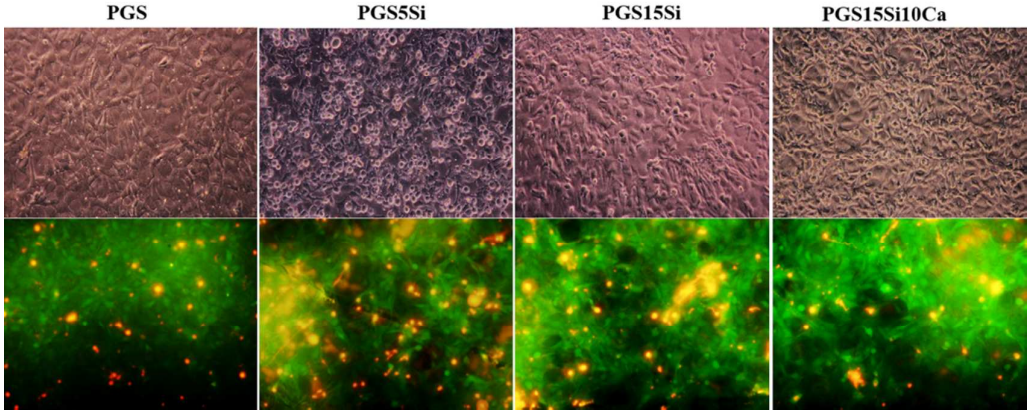

Figure 11. MC3T3 cells attachment and morphology after culture on PGS and PGSSC hybrid elastomers for 3 days (10×objective). Significantly high cell attachment was observed on the surface of samples.

4. Conclusions

In summary, we successfully fabricated highly bioactive and degradable PGSSC hybrid elastomers by conventional solution-based hybridization method. PGSSC elastomers showed representative elastic behavior and highly tunable mechanical properties (tensile strength and modulus) which were significantly higher than PGS elastomers. Significantly enhanced hydrophilicity and degradation were also observed for PGSSC hybrid

elastomers compared with PGS. In addition, PGSSC demonstrated significantly high biomineralization activity and osteoblast biocompatibility in contrast to pure PGS elastomers. The novel hybrid structure and properties make our PGSSC hybrid elastomers promising for bone tissue regeneration applications.

Acknowlegements

We acknowledge the valuable comments of potential reviewers. This work was supported by the scientific research starting foundationfrom Xi'an Jiaotong University, the Fundamental ResearchFunds for the Central Universities (XJJ2014090).

References

1. C. G. Jeong and S. J. Hollister, *Journal of Biomedical Materials Research Part B: Applied Biomaterials*, 2010, 93, 141-149.
2. C. J. Bettinger, *Macromolecular bioscience*, 2011, 11, 467-482.
3. Y. Hong, J. Guan, K. L. Fujimoto, R. Hashizume, A. L. Pelinescu and W. R. Wagner, *Biomaterials*, 2010, 31, 4249-4258.
4. Q. Chen, S. Liang and G. A. Thouas, *Progress in Polymer Science*, 2013, 38, 584-671.
5. K.-W. Lee, D. B. Stolz and Y. Wang, *Proceedings of the National Academy of Sciences*, 2011, 108, 2705-2710.
6. P. M. Crapo and Y. Wang, *Biomaterials*, 2010, 31, 1626-1635.
7. C. A. Sundback, J. Y. Shyu, Y. Wang, W. C. Faquin, R. S. Langer, J. P. Vacanti and T. A. Hadlock, *Biomaterials*, 2005, 26, 5454-5464.
8. R. Rai, M. Tallawi, A. Grigore and A. R. Boccaccini, *Progress in Polymer Science*, 2012, 37, 1051-1078.
9. Q.-Z. Chen, A. Bismarck, U. Hansen, S. Junaid, M. Q. Tran, S. E. Harding, N. N. Ali and A. R. Boccaccini, *Biomaterials*, 2008, 29, 47-57.
10. L. Quan-Yong, W. Si-Zhu, T. Tian-Wei, W. Jing-Yi, Z. Li-Qun, L. Li, T. Wei and C. Da-Fu, *Journal of Biomaterials Science, Polymer Edition*, 2009, 20, 1567-1578.
11. Q.-Z. Chen, S.-L. Liang, J. Wang and G. P. Simon, *Journal of the mechanical behavior of biomedical materials*, 2011, 4, 1805-1818.
12. Y. Wu, R. Shi, D. Chen, L. Zhang and W. Tian, *Journal of Applied Polymer Science*, 2012, 123, 1612-1620.
13. Q. Chen, C. Zhu, G. A. Thouas, R. Kengne-Momo, F. Lagarde, P. Daniel, J. Pilard and M. Durand, *Progress in Biomaterials*, 2012, 1, 2.
14. C. Zhao, W. Ji, P. Han, J. Zhang, Y. Jiang and X. Zhang, *Journal of Nanoparticle Research*, 2011, 13, 645-654.
15. M. Raucci, V. D'Antò, V. Guarino, E. Sardella, S. Zeppetelli, P. Favia and L. Ambrosio, *Acta biomaterialia*, 2010, 6, 4090-4099.
16. S. Bose, M. Roy and A. Bandyopadhyay, *Trends in biotechnology*, 2012, 30, 546-554.
17. A. Hoppe, N. S. Güldal and A. R. Boccaccini, *Biomaterials*, 2011, 32, 2757-2774.
18. B. Lei, X. Chen and Y.-H. Koh, *Journal of sol-gel science and technology*, 2011, 58, 656-663.
19. C. Przybylowski, T. Quinn, A. Callahan, M. Kaplan, A. Golding, C. Alesi, M. Ammar, C. E. LeBlon, Y. Guo and X. Zhang, *Journal of Materials Chemistry*, 2012, 22, 10672-10683.

20. A. Rainer, S. M. Giannitelli, F. Abbruzzese, E. Traversa, S. Licoccia and M. Trombetta, *Acta biomaterialia*, 2008, 4, 362-369.
21. D. Arcos and M. Vallet-Regí, *Acta Biomaterialia*, 2010, 6, 2874-2888.
22. A. Feinle, F. Lavoie-Cardinal, J. Akbarzadeh, H. Peterlik, M. Adlung, C. Wickleder and N. Hüsing, *Chemistry of Materials*, 2012, 24, 3674-3683.
23. J. Pawlik, M. Widziołek, K. Cholewa‐Kowalska, M. Łączka and A. M. Osyczka, *Journal of Biomedical Materials Research Part A*, 2014, 102, 2383-2394.
24. X. Chen, C. Guo and N. Zhao, *Applied Surface Science*, 2008, 255, 466-468.
25. T. Qu and X. Liu, *Journal of Materials Chemistry B*, 2013, 1, 4764-4772.
26. B. Lei, L. Wang, X. Chen and S.-K. Chae, *Journal of Materials Chemistry B*, 2013, 1, 5153-5162.
27. L. Ci and J. Bai, *Advanced Materials*, 2004, 16, 2021-2024.
28. B. Lei, X. Chen, X. Han and J. Zhou, *Journal of Materials Chemistry*, 2012, 22, 16906-16913.
29. B. Lei, X. Chen, Y. Wang, N. Zhao, C. Du and L. Fang, *Biomedical Materials*, 2010, 5, 054103.
30. J. R. Jones, *Acta biomaterialia*, 2013, 9, 4457-4486.
31. B. A. Allo, A. S. Rizkalla and K. Mequanint, *Langmuir*, 2010, 26, 18340-18348.
32. O. Mahony, O. Tsigkou, C. Ionescu, C. Minelli, L. Ling, R. Hanly, M. E. Smith, M. M. Stevens and J. R. Jones, *Advanced Functional Materials*, 2010, 20, 3835-3845.
33. I. Shabani, V. Haddadi-Asl, M. Soleimani, E. Seyedjafari, F. Babaeijandaghi and N. Ahmadbeigi, *Tissue Engineering Part A*, 2011, 17, 1209-1218.
34. M. Honda, K. Kikushima, Y. Kawanobe, T. Konishi, M. Mizumoto and M. Aizawa, *Journal of Materials Science: Materials in Medicine*, 2012, 23, 2923-2932.
35. S. Heinemann, C. Heinemann, S. Wenisch, V. Alt, H. Worch and T. Hanke, *Acta biomaterialia*, 2013, 9, 4878-4888.
36. B. Lei, K.-H. Shin, D.-Y. Noh, I.-H. Jo, Y.-H. Koh, W.-Y. Choi and H.-E. Kim, *Journal of Materials Chemistry*, 2012, 22, 14133-14140.
37. A. Patel, A. K. Gaharwar, G. Iviglia, H. Zhang, S. Mukundan, S. M. Mihaila, D. Demarchi and A. Khademhosseini, *Biomaterials*, 2013, 34, 3970-3983.
38. Z. Wang, B. Xu, L. Zhang, J. Zhang, T. Ma, J. Zhang, X. Fu and W. Tian, *Nanoscale*, 2013, 5, 2065-2072.
39. H. Xing, W. Bu, S. Zhang, X. Zheng, M. Li, F. Chen, Q. He, L. Zhou, W. Peng and Y. Hua, *Biomaterials*, 2012, 33, 1079-1089.
40. Y. Wang, G. A. Ameer, B. J. Sheppard and R. Langer, *Nature biotechnology*, 2002, 20, 602-606.
41. S. Salehi, T. Bahners, J. Gutmann, S.-L. Gao, E. Mäder and T. Fuchsluger, *RSC Advances*, 2014, 4, 16951-16957.
42. G. W. Ehrenstein, G. Riedel and P. Trawiel, *Thermal analysis of plastics: theory and practice*, Carl Hanser Verlag GmbH Co KG, 2012.
43. B. P. Tripathi and V. K. Shahi, *Progress in Polymer Science*, 2011, 36, 945-979.
44. S.-L. Liang, W. D. Cook, G. A. Thouas and Q.-Z. Chen, *Biomaterials*, 2010, 31, 8516-8529.
45. R. Kasemann and H. K. Schmidt, 2010.
46. Z. Chen, X. Mo, C. He and H. Wang, *Carbohydrate Polymers*, 2008, 72, 410-418.
47. I. Armentano, M. Dottori, E. Fortunati, S. Mattioli and J. Kenny, *Polymer degradation and stability*, 2010, 95, 2126-2146.
48. M. N. Collins and C. Birkinshaw, *Carbohydrate polymers*, 2013, 92, 1262-1279.
49. E. García‐Gareta, J. Hua and G. W. Blunn, *Journal of Biomedical Materials Research Part A*, 2014.
50. W. M. van Hout, A. B. M. van der Molen, C. C. Breugem, R. Koole and E. M. Van Cann, *Clinical oral investigations*, 2011, 15, 297-303.

51. S.-H. Jun, E.-J. Lee, S.-W. Yook, H.-E. Kim, H.-W. Kim and Y.-H. Koh, *Acta biomaterialia*, 2010, 6, 302-307.

52. Ł. John, M. Bałtrukiewicz, P. Sobota, R. Brykner, Ł. Cwynar-Zając and P. Dzięgiel, *Materials Science and Engineering: C*, 2012, 32, 1849-1858.

53. R. Nirmala, K. T. Nam, D. K. Park, B. Woo-il, R. Navamathavan and H. Y. Kim, *Surface and Coatings Technology*, 2010, 205, 174-181.

Table of Content:

A highly bioactive and biodegradable PGS-Silica bioactive glass hybrid elatomer with tailored mechanical properties were developed for bone tissue regeneration application